

Anion-Perturbed Magnetic Slow Relaxation in Planar {Dy₄} Clusters

Yan-Zhen Zheng, Yanhua Lan, Christopher E. Anson, and Annie K. Powell*

Institut für Anorganische Chemie, Universität Karlsruhe (TH), Engesserstrasse Geb. 30.45, 76128 Karlsruhe, Germany

Received September 1, 2008

Two planar tetranuclear dysprosium(III) complexes, [Dy₄(μ₃-OH)₂-(hmpH)₂(hmp)₂(Cl)₄]·3MeCN·MeOH (**1**) and [Dy₄(μ₃-OH)₂-(hmpH)₂(hmp)₂(N₃)₄]·4MeOH (**2**) {hmpH₂ = 2-[(2-hydroxyethylimino)methyl]-6-methoxyphenol}, which exhibit an anion-dependent magnetic slow relaxation behavior, have been synthesized by in situ condensation of *o*-vanillin and 2-aminoethanol. The higher energy barrier observed in **2** could be the result of a more favorable crystal field and/or orientations of single-ion easy axes of magnetization of the Dy^{III} ions.

The discovery of single molecule magnets (SMMs)¹ opened a new page in modern coordination chemistry with the promise of a revolution in data storage and processing.² Up to now, the “best” SMMs are all manganese clusters, in particular Mn₁₂ and Mn₆,³ which hold the highest energy barriers to reversal of spin so far reported. The barrier can be related to the uniaxial anisotropy, in the case of Mn^{III}, for example, *D*, the axial zero-field-splitting (ZFS) parameter, and to the square of the ground spin state, *S*. However, it has proved remarkably difficult to optimize both parameters, and the blocking temperatures of all of the SMMs so far discovered are still very low, placing a limit on the usefulness of their extensive possible applications.

Although the spin can be successfully maximized by finding systems that are ferromagnetically coupled,⁴ maximizing *D* (while preventing higher ZFS parameters from becoming significant) represents a major challenge.⁵ Thus, after the discovery of many 3d transition-metal-based SMMs, interest has been reawakened in the area of 3d–4f metal

clusters⁶ as well as pure 4f metal systems⁷ in the search for new SMMs. Although the magnetic coupling in these systems is likely to be small, the large magnetic anisotropy of lanthanides such as Dy^{III}, Tb^{III}, and Ho^{III}⁸ means that 3d–4f or 4f metal-based SMMs could possess larger energy barriers provided the magnetic principal axes of these ions are properly oriented. Interestingly, even mononuclear complexes of Dy^{III}, Tb^{III}, and Ho^{III} can show strong slow relaxation behavior at relatively high temperatures,⁹ which may indicate that the ligand (or electric) field is another key player in controlling the magnetic anisotropy of lanthanide-based SMMs.⁸ However, far fewer 4f SMMs have so far been reported compared to those based on 3d metals.³

Recently, we reported two unusual Dy^{III} compounds, [Dy₃(μ₃-OH)₂L₃Cl₂(H₂O)₄][Dy₃(μ₃-OH)₂(van)₃Cl(H₂O)₅] Cl₅·19H₂O and [Dy₃(μ₃-OH)₂(van)₃Cl(H₂O)₅] Cl₃·4H₂O·2MeOH·0.7MeCN (van = *o*-vanillato),⁷ which have similar Dy^{III}₃ triangles and are denoted as {Dy^{III}₃} hereafter. Surprisingly, {Dy^{III}₃} has an almost diamagnetic ground spin state but shows strong slow relaxation behavior within the excited states. This intriguing magnetic behavior is mainly the result of the noncollinearity of the single-ion easy axes of magnetization of the Dy^{III} ions, which lie in the plane of the triangle at 120° to each other, leading to the peculiar chiral nature of the ground nonmagnetic doublet.^{10,11} Such systems with a nonmagnetic ground doublet state could be used, for example, to reduce decoherence effects due to the fluctuation

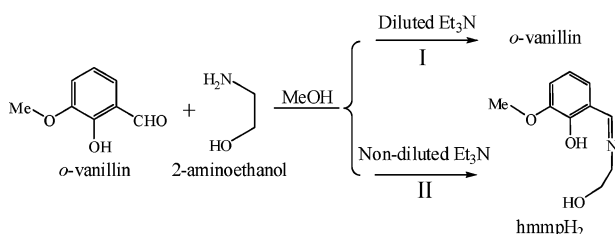
* To whom correspondence should be addressed. E-mail: powell@aoc.uni-karlsruhe.de. Fax: +49-721-6088142.

- (1) Sessoli, R.; Gatteschi, D.; Caneschi, A.; Novak, M. A. *Nature* **1993**, *365*, 141.
- (2) Leuenberger, M. N.; Loss, D. *Nature* **2001**, *410*, 789.
- (3) For reviews, see: (a) Christou, G.; Gatteschi, D.; Hendrickson, D. N.; Sessoli, R. *MRS Bull.* **2000**, *25*, 66. (b) Gatteschi, D.; Sessoli, R. *Angew. Chem., Int. Ed.* **2003**, *43*, 268. (c) Aromí, G.; Brechin, E. K. *Struct. Bonding (Berlin)* **2006**, *122*, 1.
- (4) Ako, A. M.; Hewitt, I. J.; Mereacre, V.; Clérac, R.; Wernsdorfer, W.; Anson, C. E.; Powell, A. K. *Angew. Chem., Int. Ed.* **2006**, *45*, 4926.
- (5) (a) Waldmann, O. *Inorg. Chem.* **2007**, *46*, 10035. (b) Ruiz, E.; Cirera, J.; Cano, J.; Alvarez, S.; Loosec, C.; Kortus, J. *Chem. Commun.* **2008**, *52*.

- (6) (a) Osa, S.; Kido, T.; Matsumoto, N.; Re, N.; Pochaba, A.; Mrozinski, J. *J. Am. Chem. Soc.* **2004**, *126*, 420. (b) Zaleski, C. M.; Depperman, E. C.; Kampf, J. W.; Kirk, M. L.; Pecoraro, V. L. *Angew. Chem., Int. Ed.* **2004**, *43*, 3912. (c) Schelter, E. J.; Prosvirin, A. V.; Dunbar, K. R. *J. Am. Chem. Soc.* **2004**, *126*, 15044. (d) Mereacre, V.; Ako, A. M.; Clérac, R.; Wernsdorfer, W.; Filoti, G.; Bartolomé, J.; Anson, C. E.; Powell, A. K. *J. Am. Chem. Soc.* **2007**, *129*, 9248. (e) Mereacre, V.; Ako, A. M.; Clérac, R.; Wernsdorfer, W.; Hewitt, I. J.; Anson, C. E.; Powell, A. K. *Chem.—Eur. J.* **2008**, *45*, 707.
- (7) Tang, J.; Hewitt, I.; Madhu, N. T.; Chastanet, G.; Wernsdorfer, W.; Anson, C. E.; Benelli, C.; Sessoli, R.; Powell, A. K. *Angew. Chem., Int. Ed.* **2006**, *45*, 1729.
- (8) Benelli, C.; Gatteschi, D. *Chem. Rev.* **2002**, *102*, 2369.
- (9) (a) Ishikawa, N.; Sugita, M.; Wernsdorfer, W. *J. Am. Chem. Soc.* **2005**, *127*, 3650. (b) Ishikawa, N.; Sugita, M.; Wernsdorfer, W. *Angew. Chem., Int. Ed.* **2005**, *44*, 2931. (c) Takamatsu, S.; Ishikawa, T.; Koshihara, S.-y.; Ishikawa, N. *Inorg. Chem.* **2007**, *46*, 7250.
- (10) Chibotaru, L. F.; Ungur, L.; Soncini, A. *Angew. Chem., Int. Ed.* **2008**, *47*, 4126.
- (11) Luzon, J.; Bernot, K.; Hewitt, I. J.; Anson, C. E.; Powell, A. K.; Sessoli, R. *Phys. Rev. Lett.* **2008**, *100*, 247205/1–247205/4.

COMMUNICATION

Scheme 1. Reaction Results (Et₃N = triethylamine)



of local magnetic fields. Thus, such a planar spin noncollinearity effect is interesting and important in the area of molecular magnetism, stimulating further investigation in related planar compounds.^{10,11}

The synthesis of the {Dy^{III}}_3 compounds used a reaction designed to lead to the in situ formation of a Schiff base as a ligand. In the event, however, the *o*-vanillin did not condense with 2-aminoethanol under the slow addition of dilute triethylamine; the latter probably merely acts to optimize the pH for the successful isolation of the compound. We now find that simply by adding nondiluted triethylamine quickly¹² the desired condensation products form and act as ligands in the compounds [Dy₄(μ₃-OH)₂(hmmpH)₂(hmmp)₂(Cl)₄]·3MeOH·MeCN (**1**) and [Dy₄(μ₃-OH)₂(hmmpH)₂(hmmp)₂(N₃)₄]·4MeOH (**2**) {where hmmpH₂ = 2-[(2-hydroxyethylimino)methyl]-6-methoxyphenol; see Scheme 1}. These two compounds have planar cores of four Dy^{III} ions, which can be regarded as the fusion of two triangles. They show slow relaxation of the magnetization, albeit at lower temperatures than those seen for {Dy^{III}}_3.

Single-crystal X-ray diffraction studies¹³ reveal that the core structure of **1** has a tetranuclear arrangement of Dy^{III} ions with crystallographic inversion symmetry. In contrast with most tetranuclear compounds,³ the four Dy^{III} ions are precisely coplanar, as shown in Figure 1. The two oxygen atoms (O1) of the μ₃-OH ligands are located on opposite

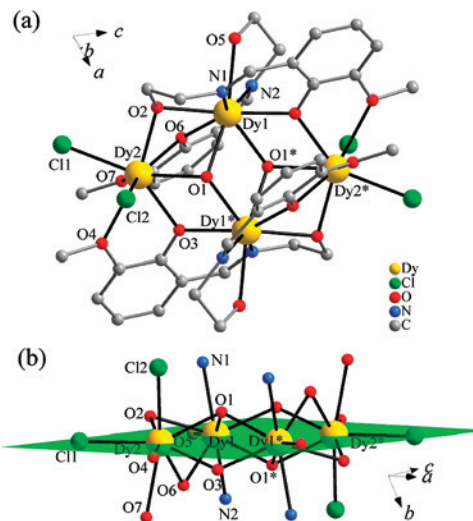
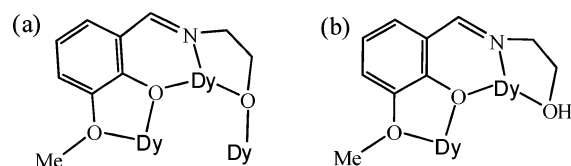


Figure 1. Perspective view (a) and side view (core only) (b) of the tetranuclear core in **1**. Atoms marked with asterisks are inversion-center-generated.

Scheme 2. Coordination Modes of hmmp (a) and hmmpH (b)



sides of the Dy₄ plane and are displaced out of that plane by 0.922 Å. The hydroxo forms a fairly symmetrical triple bridge, with the Dy–O1 distances 2.344(3), 2.347(3), and 2.381(3) Å and the Dy–O1–Dy angles 95.16(12), 110.71(13), and 111.01(13)°. Dy1 is chelated by the two independent organic ligands via the imino nitrogen and the phenoxy and alcohol oxygen atoms, and these connect to Dy2/Dy2*. The coordination and bridging modes of the ligands are shown in Scheme 2. The Dy–O bond lengths are in the range 2.314(3)–2.555(4) Å, with the deprotonated oxygen atoms making shorter bonds. The Dy–N bond lengths are 2.471(4) and 2.480(4) Å, while the Dy2–Cl distances are 2.6517(13) and 2.6901(17) Å. While the hmmpH₂ ligand is known in 3d transition-metal complexes, this is the first example of its use for 4f coordination chemistry.

The structure of **2** is essentially isomorphous to **1**, with the chlorides in **1** having been replaced by azides, as shown in Figure S1 in the Supporting Information. The Dy–N(azide) distances are, as expected, shorter than those for the chlorides, at 2.354(6) and 2.369(5) Å. Apart from this change, there is no clear change to the cluster geometry, with Dy–X distances not changing significantly. There is almost negligible twisting of the ligands between **1** and **2**, but this is unlikely to have any significant effect on the magnetic properties. In both compounds, the two crystallographically independent ions, Dy1 and Dy2, are eight-coordinate, displaying a distorted square-antiprismatic geometry. It is tempting to imagine that the 4-fold axes of the square antiprisms might correspond to the magnetic easy axes of the Dy^{III} ions. However, the eight-coordinating atoms are not equivalent, with some “harder” (hydroxo, alkoxo, and phenoxy) than others (neutral oxygens, azide, and chloride).

(12) **1** was prepared by quickly adding triethylamine (1.0 mmol) to a stirred solution of DyCl₃·6H₂O (1.0 mmol), *o*-vanillin (1.0 mmol), and 2-aminoethanol (1.0 mmol) in 40 mL of a 3:1 MeOH/MeCN mixture. After slow evaporation over 2 weeks, the yellow solution yielded X-ray-quality yellow block crystals. Yield: 140 mg/ 31.2%. Anal. Calcd for **1**·7H₂O: C, 27.83; H, 3.62; N, 3.24. Found: C, 27.78; H, 3.24; N, 3.74. IR (KBr disk, cm⁻¹): 3429 (br), 1639 (vs), 1555.6 (m), 1448 (s), 1411 (m), 1303 (m), 1216 (s), 1096 (w), 949 (m), 859 (w), 788 (w), 729 (m), 649 (w), 553 (w). Pale-yellow plates of **2** result if 10 mL of a saturated methanolic solution of NaN₃ is added to the reaction mixture. Yield: 60 mg/13.7%. Anal. Calcd for **2**·4H₂O: C, 28.28; H, 3.32; N, 13.19. Found: C, 28.23; H, 3.14; N, 12.85. IR (KBr disk, cm⁻¹): 3410 (br), 2087 (vs), 1635 (s), 1555 (w), 1471 (s), 1393 (w), 1301 (w), 1221 (s), 1053 (m), 961 (m), 894 (w), 856 (w), 787 (w), 738 (m), 629 (w), 563 (w).

(13) Crystal data for **1**: C₄₉H₇₃Cl₄Dy₄N₇O₁₇, *M* = 1823.94 g mol⁻¹, triclinic, space group *P* $\bar{1}$, *T* = 200 K, *a* = 11.2208(14) Å, *b* = 11.9345(15) Å, *c* = 14.1452(18) Å, α = 87.530(15)°, β = 66.880(14)°, γ = 63.590(14)°, *V* = 1540.3(3) Å³, *Z* = 1, *F*(000) = 884, ρ = 1.966 g cm⁻³, μ = 5.039 mm⁻¹; total data 11 187, unique data 5631, *R*_{int} = 0.0408, 372 parameters, *wR*² = 0.0984, *S* = 1.000 (all data), *R*₁ = 0.0352 for 4885 with *I* ≥ 2σ(*I*), largest diff peak/hole +0.90/−0.73 e Å⁻³. Crystal data for **2**: C₄₄H₆₄Dy₄N₁₆O₁₈, *M* = 1755.11 g mol⁻¹, triclinic, space group *P* $\bar{1}$, *T* = 100 K, *a* = 11.1847(5) Å, *b* = 11.3918(5) Å, *c* = 13.8717(6) Å, α = 81.061(1)°, β = 66.851(1)°, γ = 63.009(1)°, *V* = 1447.6(1) Å³, *Z* = 1, *F*(000) = 848, ρ = 2.013 g cm⁻³, μ = 5.184 mm⁻¹; total data 8425, unique data 5396, *R*_{int} = 0.0182, 382 parameters, *wR*² = 0.0785, *S* = 1.079 (all data), *R*₁ = 0.0340 for 4986 with *I* ≥ 2σ(*I*), largest diff peak/hole +1.74/−0.75 e Å⁻³. Crystallographic data (excluding structure factors) are available from the Cambridge Crystallographic Data Centre as supplementary publication nos. CCDC 706291 and 706292.

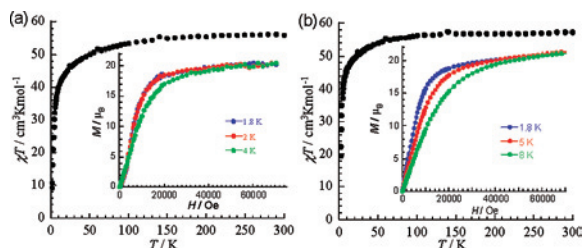


Figure 2. Plots of χT vs T at the applied field of 0.1 T of **1** (a) and **2** (b). Inset: Plots of M vs H for **1** (a) and **2** (b) at the indicated temperatures.

Furthermore, the distributions of hard and soft atoms are unsymmetrical relative to the principal axes of the antiprisms, so that it would be unwise to try to assign the directions of the easy axes.

Such tetranuclear structures are often viewed in terms of two edge-sharing triangles, which in this case are close to isosceles, because the distances for Dy1...Dy2, Dy1...Dy2*, and Dy1...Dy1* in **1** and **2** are 3.4878(14) and 3.4650(5), 3.8896(9) and 3.8693(4), 3.8662(12) and 3.8671(6) Å, respectively. The shortest edge, Dy1...Dy2, is that which involves three oxygen bridges rather than just two. We can also note that the triangles in **2** are slightly smaller than those in **1**. The Dy...Dy distances can also be compared to those in the {Dy^{III}₃} triangles (3.503–3.540 Å).

Magnetic studies were performed on polycrystalline samples of **1** and **2**. At room temperature (300 K), the χT values are 55.91 and 57.32 $\text{cm}^3 \text{K mol}^{-1}$ for **1** and **2** (Figure 2), respectively, which are close to the expected value of 56.68 $\text{cm}^3 \text{K mol}^{-1}$ for a Dy^{III}₄ unit ($S = 5/2$, $L = 5$, $g = 4/3$, ${}^6\text{H}_{15/2}$, $C = 14.17 \text{ cm}^3 \text{K mol}^{-1}$).⁷ A fit of the experimental data to a Curie–Weiss law above 30 K (Figure S2 in the Supporting Information) leads to Curie and Weiss constants of 57.56 and 57.90 $\text{cm}^3 \text{K mol}^{-1}$ and -7.35 and -3.39 K for **1** and **2**, respectively. Below 200 K, the χT value gradually decreases for **1**, whereas for **2**, the value remains unchanged until 100 K. Below 100 K, the χT plot of **1** decreases faster than that of **2**, to reach a value of 9.12 and 19.49 $\text{cm}^3 \text{K mol}^{-1}$ at 1.8 K for **1** and **2**, respectively. This indicates that the crystal field and/or the magnetic interactions between the Dy^{III} ions⁷ are different in **1** and **2**. This difference was confirmed from the field-dependent magnetization at 1.8 K (inset of Figure 2). As can be seen from the M vs H plot, up to 7 T the maximum of **2** is 22.08 μ_B and larger than that of **1**, which is 20.37 μ_B . These maxima are slightly different but in relatively good agreement with the expected value ($4 \times 5.23 \mu_B$) for four isolated Dy^{III} ions. The lack of saturation on the M vs H data at 1.8 K suggests the presence of significant anisotropy and/or low-lying excited states, in agreement with weak intracomplex interactions also suggested by the χT vs T data and the small Weiss constants.

Moreover, the χT values from 15 to 2 K are virtually identical with the $\chi' T$ values obtained from the temperature-dependent in-phase (χ') alternating current (ac) magnetic

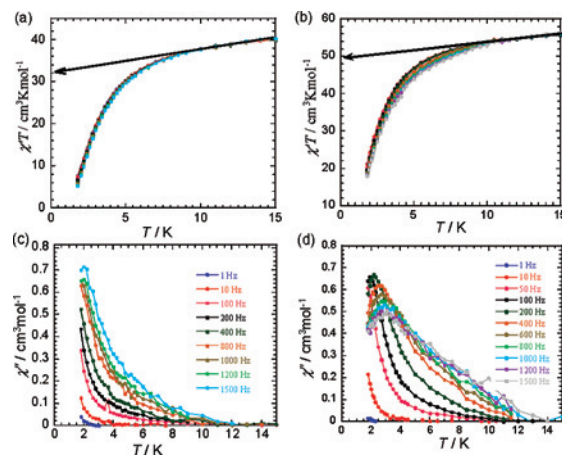


Figure 3. Temperature dependence of the in-phase (a and b for **1** and **2**, respectively) and out-of-phase (c and d for **1** and **2**, respectively) ac susceptibilities at the indicated frequencies.

susceptibility (Figure 3). The extrapolation of $\chi' T$ to the intersections of the Y axes might indicate that **1** and **2** have different ground spin states. However, we cannot safely correlate which spin states **1** and **2** have simply according to these $\chi' T$ values.

The out-of-phase (χ'') ac magnetic susceptibility signals also show different magnetic slow relaxation behavior for **1** and **2**. For **1**, the maxima of χ'' cannot be observed even up to 1500 Hz. However, for **2**, the maxima of χ'' are clearly observed from 100 to 1500 Hz. Hence, the energy barrier and characteristic relaxation time of the system can be obtained by fitting the peak temperatures with the Arrhenius law [$\tau = \tau_0 \exp(U_{\text{eff}}/k_B T)$], giving $U_{\text{eff}} = 7.0(1)$ K and $\tau_0 = 3.8 \times 10^{-5}$ s (Figure S3 in the Supporting Information).

The different slow relaxation behaviors seen in **1** and **2** are probably the result of the slight changes in the structure, which are likely to affect the nature or directions of the easy axes through the ligand fields of the terminal anions.^{10,11} Because of the challenges in describing the crystal field of Dy^{III}, it is difficult to make any further comment on this except to note that the observation that the magnetic slow relaxation behavior is directly influenced by the nature of the anion, which provides an opportunity to shed light on tuning of the magnetic properties of SMMs.

Acknowledgment. This work was supported by the DFG (CFN and SPP 1137), MAGMANet (Grant NMP3-CT-2005-515767), and the Alexander von Humboldt Foundation (to Y.-Z.Z.).

Supporting Information Available: Experimental details, crystal data (CIF file, additional structural data and plots), and additional magnetic data. This material is available free of charge via the Internet at <http://pubs.acs.org>.

IC8016722